A Low-Profile Spilt Ring Monopole Antenna Loaded with Hexagonal Split Ring Resonator for RFID Applications

Rapheal Samson Daniel[*] and Rajapriya Selvaraj

Abstract—This article describes a compact split ring monopole antenna loaded with a Hexagonal Split Ring Resonator (Hex-SRR) for Wireless Local Area Network (WLAN) and Radio frequency Identification (RFID) applications. The resonance frequency of the proposed antenna is obtained by making use of a split ring structure and a metamaterial element Hex-SRR. The prototype antenna is printed on an FR-4 substrate having a dielectric constant (ε_r) of 4.4 with dimensions of $21 \times 21 \times 1.6 \, \text{mm}^3$. The split in the ring radiating element is used to achieve good impedance matching, and the Hex-SRR creates a new resonance frequency of 5.8 GHz. This paper includes equivalent circuit investigation, operating mechanism, and band characteristics of Hex-SRR as well as negative permeability details. The fabricated antenna provides an impedance bandwidth of 1180 MHz (5.23–6.41 GHz), which is suitable for WLAN and RFID applications. Good similarity is inferred between the simulated and measured results of the proposed antenna.

1. INTRODUCTION

Broadband monopole antenna is an embryonic necessity in the field of wireless communications. The frequency spectrum employed by the IEEE 802.11a for a WLAN system is 5.15–5.35 GHz and 5.725–5.825 GHz. Numerous techniques have been devised to realize wide bandwidth and good impedance matching. In general, the bandwidth of the antenna has been improved by fractal theory [1], symmetrical stubs [2], and parasitic element [3] in the radiating element.

Recent studies have proved that metamaterial antennas have been used for improving antenna characteristics due to negative values of permittivity and permeability from its structural arrangement of unit cells. This unusual property is not found in natural materials [4]. Split Ring Resonator (SRR) is a class of metamaterial element, which has quasi-static resonant nature due to inductance and capacitance of the ring and split gap [5]. Due to sub-wavelength nature, SRR has been used to reduce the antenna size [6] and improve bandwidth [7]. Triangle SRR (TSRR) radiating structure has been analyzed in attaining good impedance matching [8]. Negative Refractive Index-Transmission Line [9] supports the metamaterial characteristics due to its shunt inductance and series capacitance for achieving wider impedance bandwidth. An inclusion of a split ring structure in radiating element [10] exhibits better impedance matching.

In this article, a compact metamaterial inspired split ring monopole antenna loaded with a Hex-SRR is proposed for 5.8 GHz RFID applications. The new resonance frequency is achieved by introducing a Hex-SRR in the split ring radiating element, which is investigated by equivalent circuit model with empirical design formulas. Hex-SRR resonance frequency and its permeability characteristics are also studied to validate the results.

2. PROPOSED ANTENNA STRUCTURE AND ITS SIMULATED RESULTS

The design methodology of the proposed antenna is shown in Fig. 1(a). Prototype A illustrates a hexagonal ring radiating structure and has a partial ground plane. This structure is utilized to realize a resonance frequency of 6 GHz. This resonant frequency is calculated by [13, 14],

$$f_r = \frac{1.8412 \times c}{2\pi S \sqrt{\varepsilon_r}} = \frac{1.8412 \times 3 \times 10^8}{2 \times 3.14 \times 7 \times 10^{-3} \sqrt{4.4}} = 6\,\text{GHz} \tag{1}$$

Here, ε_r is the dielectric constant of the FR-4 substrate and side length of the hexagonal ring radiating element $S = 7\,\text{mm}$. Hence, the side of hexagonal length 7 mm yields a resonance frequency of 6 GHz. In prototype B, a split is created at the top of the hexagonal ring, which is used to generate magnetic resonance and leads to good impedance matching due to its gap capacitance of the split resonator. The split is placed at the center of the hexagonal ring to maintain symmetry and ensure design simplicity. As shown in prototype C, a Hex-SRR is created in the center of the split ring radiating structure at a distance (d_1) of 7.3 mm ($\lambda_g/3.38$) from the bottom of the microstrip for obtaining better impedance matching and bandwidth improvement. It modifies the current distribution of the split ring radiating structure and produces a quarter wavelength resonances at 5.8 GHz.

Figure 1. Design steps of the proposed antenna.

The pictorial representation of the antenna geometry is depicted in Fig. 2, and its values are detailed in Table 1. A photograph of the fabricated structure is exposed in Fig. 3.
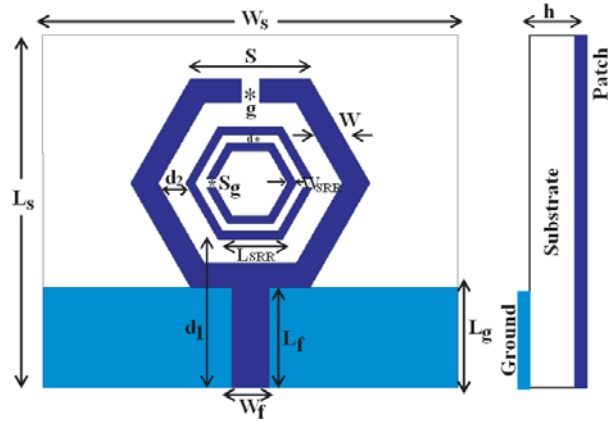

Figure 2. Pictorial representation of the antenna geometry. (a) Top view and (b) side view.

Simulations are performed using Ansys HFSS V.14.0 EM software package. The evaluation of simulated S_{11} (dB) of three prototypes are depicted in Fig. 4. As the figure represents, prototype A has an impedance bandwidth of 1390 MHz (5.29–6.68 GHz) with a resonance frequency of 6 GHz. When the split is influenced in the ring radiating element (prototype B), better impedance matching has been observed. Here, the resonant frequency is shifted from 6 GHz to 5.95 GHz. In prototype C, a Hex-SRR is introduced inside the split ring radiating element. It effectively changes the current path of split ring
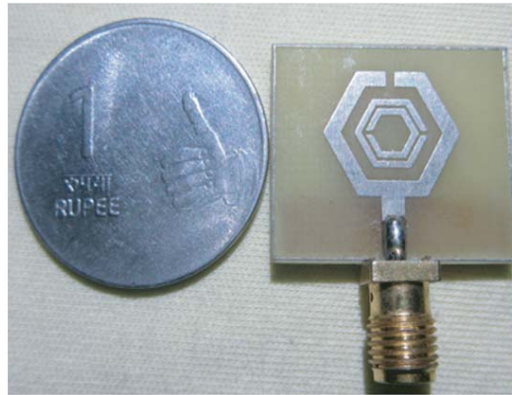
Figure 3. Proposed antenna fabricated structure.

Table 1. Dimensions of the proposed antenna.

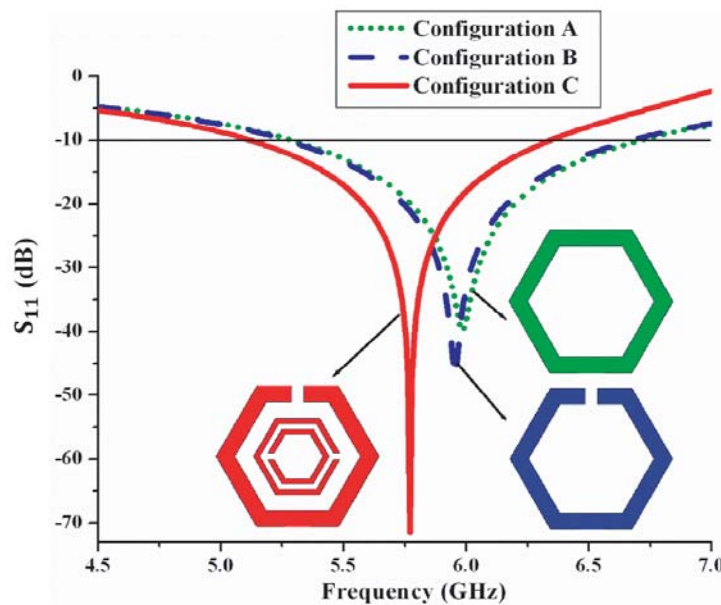| Parameter	Dimension (mm)	Parameter	Dimension (mm)
W_s	22.64	L_g	5.51
L_s	19.18	S	7
W_f	2	W	1.5
L_f	5.51	d	0.5
W_{SRR}	0.5	d_1	7.3
L_{SRR}	3.5	d_2	1.5
g	1	s_g	0.5

Figure 4. Return loss characteristics of the prototypes A, B, and C.

radiating element and leads to better impedance matching. Also, it is found that there is a change in resonant frequency of 5.95 GHz to 5.8 GHz due to its quarter wavelength resonance of Hex-SRR. Thus the side length of the Hex-SRR is slightly larger than quarter wavelength at 5.8 GHz (i.e., TM_{10} mode).

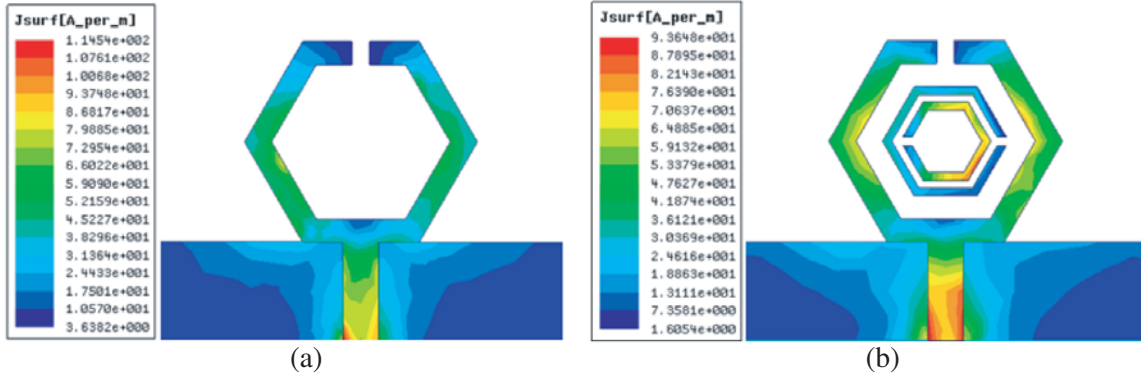(a)   (b)

Figure 5. Surface current density of (a) unloaded Hex-SRR and (b) loaded Hex-SRR at 5.8 GHz.

The proposed antenna exhibits broad bandwidth of 1230 MHz (5.13–6.36 GHz) with center frequency of 5.8 GHz, which is used to cover WLAN/RFID frequency bands.

The simulated surface current densities of unloaded and loaded Hex-SRR are shown in Figs. 5(a) and 5(b). Fig. 5(b) indicates that the Hex-SRR loaded split ring monopole makes significant current concentration around the split ring radiating element and the feed line of the monopole. Thus, Hex-SRR induces magnetic resonance and creates a new resonance frequency of 5.8 GHz for RFID applications.

3. EQUIVALENT CIRCUIT ANALYSIS OF HEXAGONAL SRR

The proposed antenna and its equivalent circuit model [11] are shown in Fig. 6. It has two metallic rings with a split. The split on the metallic position forces the electric current from one ring to another ring, to form a strong displacement current along the loop and generate equivalent magnetic dipole moment. Hence, the negative permeability property is due to the magnetic dipole moment. The distributed capacitance ($C_0/2$) is due to the split, and inductance (L_s) effect is due to the metal ring.
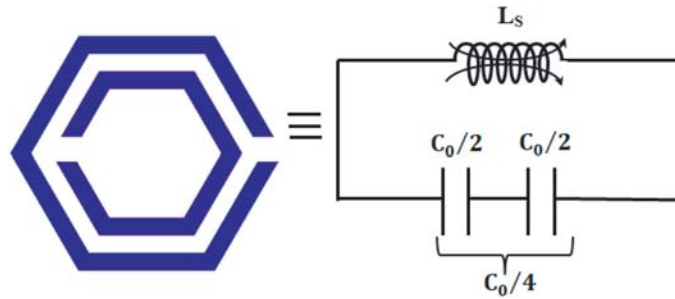

Figure 6. Equivalent circuit model.

Hence the proposed antenna resonance frequency has been evaluated by inductance and capacitance values through MATLAB program [11].

$$f_{\mathrm{SRR}} = \frac{1}{2\pi\sqrt{L_{\mathrm{SRR}}C_{\mathrm{SRR}}}} \tag{2}$$

$$C_{\mathrm{SRR}} = \frac{N-1}{2}[2L - (2N-1)(W+S)]C_0$$

$$C_0 = \varepsilon_0\frac{K(\sqrt{1-K^2})}{K(k)} \quad \text{and} \quad k = \frac{S/2}{W+S/2}$$

$$L_{\mathrm{SRR}} = 4\mu_0[L - (N-1)(S+W)]\left[\ln\left(\frac{0.98}{\rho}\right) + 1.84\rho\right]$$

$$\rho = \frac{(N-1)(W+S)}{1-(N-1)(W+S)}$$

Where $L = 7\,\text{mm}$ is the hexagonal side length, $N = 2$ the number of Hex-SRR, $W = 0.5$ the width of the Hex-SRR, $K(k)$ the first kind elliptic integral identity, and $S = 0.5\,\text{mm}$ the distance between two Hex-SRR. Hence, $L_{\text{SRR}} = 1.7815 \times 10^{-08}$ Henry and $C_{\text{SRR}} = 4.2641 \times 10^{-14}$ Farad. Therefore, the resonance frequency is $f_{\text{SRR}} = \frac{1}{2\pi\sqrt{L_{\text{SRR}}C_{\text{SRR}}}} = 5.77\,\text{GHz}$. Thus, the proposed antenna creates a resonance frequency of 5.77 GHz, which is examined by empirical design equations.

4. OPERATING MECHANISM

The hexagonal ring resonator dimensions are calculated to support the fundamental radiating mode TM_{10} at 6 GHz, which is computed using cavity model by [13]

$$f_{r(mn)} = \frac{1}{2\pi\sqrt{\mu\varepsilon}}\sqrt{\left(\frac{m\pi}{L}\right)^2 + \left(\frac{n\pi}{W}\right)^2} \tag{3}$$

Here $\varepsilon = \varepsilon_0\varepsilon_{eff}$, $\mu = 4\pi \times 10^{-7}\,\text{h/m}$, $\varepsilon_0 = 8.8419 \times 10^{-12}\,\text{F/m}$, $m = 0, 1, 2 \ldots$; $n = 0, 1, 2 \ldots$, $L = W = $ Side length of the hexagonal closed ring resonator.

ε_{eff} is the effective dielectric constant and $L = W = 7\,\text{mm}$. The split ring structure offers a radiation mode TM_{10} (at 6 GHz). After introducing Hex-SRR, the resonance frequency is shifted towards lower frequency region at 5.8 GHz.

The comparative analysis of previously published results and the proposed antenna is listed in Table 2. From Table 2, it is perceived that the proposed antenna yields better radiation characteristics with small size. This paper highlights equivalent circuit analysis and band nature along with negative permeability characteristics for obtaining broad bandwidth.

Table 2. Comparative analysis of previously published results.

Year	Patch details	Size of the antenna $L \times W \,\text{mm}^2$	Resonance frequency (GHz)	Impedance Bandwidth (MHz)	Equivalent circuit and metamaterial property verification
[2]	Circular patch loaded with a partial split ring and a pair of symmetrical stubs.	30×30	2 GHz and 3.2 GHz	2100 MHz	Not Verified
[4]	NB-CSRR loaded patch antenna	29.4×26	2.7 GHz, 4.4 GHz and 5.6 GHz	1110 MHz, 630 MHz, 1270 MHz	Not Verified
[6]	Meandered CPW-fed and hexagonal split ring resonator	13×19.8	5.8 GHz	600 MHz	Not Verified
[7]	SRR loaded substrate	31×24.57	4.7 GHz	3760 MHz	Not Verified
[12]	SRR superstrate for a patch antenna	49.6×59.6	1.75 GHz	80 MHz	Not Verified
Proposed antenna	Split ring radiating structure loaded with Hex-SRR	21×21	5.8 GHz	1180 MHz	Verified

5. PARAMETRIC STUDY

Parametric investigation has been studied for obtaining good impedance matching between the split ring radiating element and Hex-SRR. The width of the split ring radiating structure 'W' is changed from 1.8 mm to 1.5 mm in steps of 0.1 mm, which is shown in Fig. 7. Decreasing 'W' value decreases the resonant frequency and offers better impedance matching. Hence, the optimum value for 'W' is fixed at 1.5 mm. Further analysis is done to obtain an optimum distance 'd_2' between the split ring radiating element and Hex-SRR. The distance 'd_2' is changed from 2.5 mm to 1.5 mm in steps of 0.5 mm, which is illustrated in Fig. 8. It is found that a good return loss characteristic is observed for 'd_2' value of
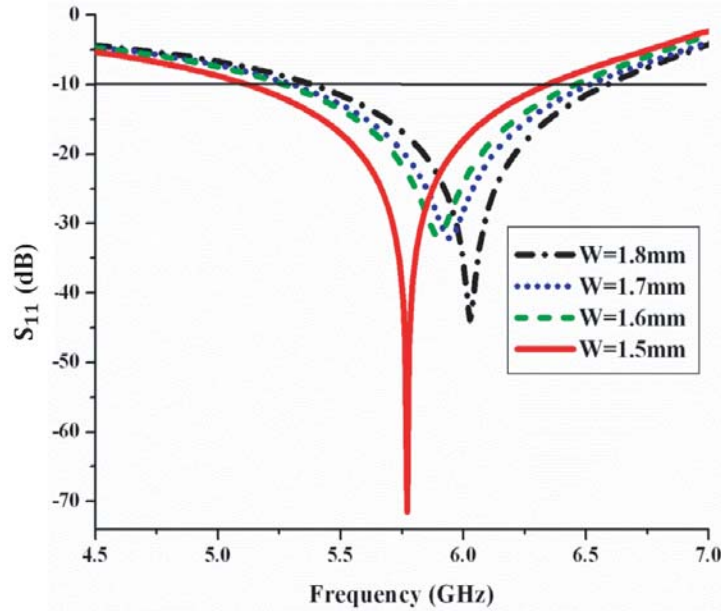

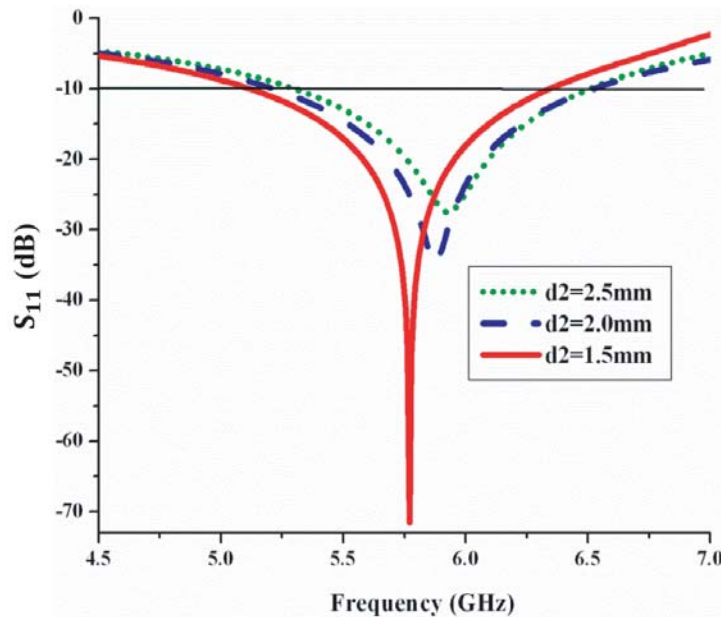**Figure 7.** Return loss for various width (W) of hexagonal ring.

Figure 8. Return loss for various distance (d_2) between the split ring structure and Hex-SRR.

1.5 mm.

Similarly, the length L_{SRR} is varied from 3.3 mm to 3.5 mm with the step of 0.1 mm, which is detailed in Fig. 9. Increasing 'L_{SRR}' value decreases the resonant frequency to realize miniaturization of the prototype antenna. Fig. 10 depicts the split effect on Hex-SRR, which is changed from 0.3 mm to 0.5 mm in steps of 0.1 mm. As the split gap (S_g) increases, the resonant frequency of the antenna decreases, and good impedance matching is obtained. Based on parametric study, the optimum values are found at $L_{SRR} = 3.5$ mm and $S_g = 0.5$ mm.
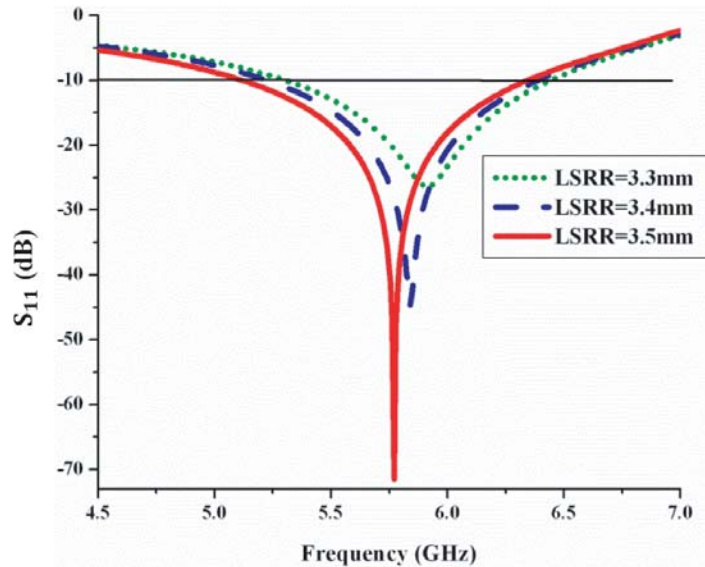

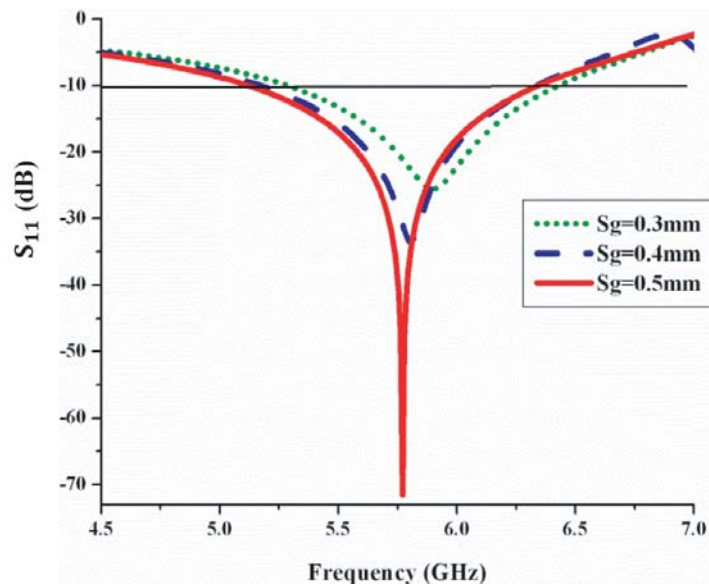**Figure 9.** S_{11} (dB) for various length (L_{SRR}) for Hex-SRR.

Figure 10. S_{11} (dB) for various split gap (S_g) of Hex-SRR.

6. RESULTS AND DISCUSSION

Anritsu Vector Network AnalyzerMS46122B is utilized to evaluate the S_{11} (dB) characteristics of the prototype antenna. The simulated and measured return losses are shown in Fig. 11. A small variation is perceived which may be due to fabrication tolerance, prototype soldering, and measurement inaccuracy. The measured data illustrate that the prototype antenna provides the -10 dB impedance bandwidth of 1180 MHz (5.23–6.41 GHz) which is useful for covering the 5.8 GHz frequency for WLAN/RFID applications. The bandwidth and impedance matching of the desired frequency range are improved using the split ring radiating element combined with metamaterial element Hex-SRR.
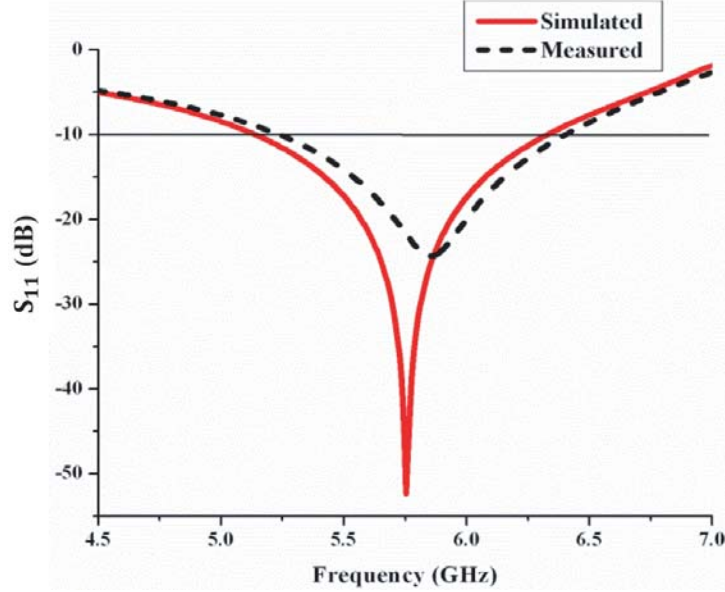

Figure 11. S_{11} (dB) characteristics of the prototype antenna.

Figure 12 illustrates the far-field radiation pattern of the proposed antenna. It exhibits a dipole radiation pattern in the elevation plane and an omnidirectional radiation pattern in the azimuthal plane at 5.8 GHz. The gain transfer method is used to measure the gain of the antenna [13], through an anechoic chamber, where the horn antenna is influenced as a reference antenna. The measured gain of the proposed antenna is shown in Fig. 13. The maximum gain value of 2.55 dBi at 5.8 GHz is observed for WLAN/RFID frequency band.

7. PARAMETER EXTRACTION OF HEX-SRR

With an inclusion of Hex-SRR based metamatrial, the new resonance frequency of 5.8 GHz is produced. This is obtained by studying the stopband and passband behaviors of Hex-SRR. The transmission coefficient (S_{21}) exhibits stopband characteristics, and reflection coefficient (S_{11}) shows passband behavior for constructing a new resonance frequency. S-parameters (S_{11} and S_{21}) of the Hex-SRR are explored and evaluated by an effective medium theory [12]. The pictorial representation of the waveguide setup is described in Fig. 14. Here, Hex-SRR is bounded by the Perfect Electric Conductor (PEC) and Perfect Magnetic Conductor (PMC) boundary conditions. Hex-SRR creates a magnetic response by an EM wave from Port 1 (input port), and S-parameters are computed from Port 2 (output port) of the waveguide.

The S-parameters are schematically represented as shown in Fig. 15. Here, the stopband is inferred around 5.3 GHz. It confirms the relation [12].

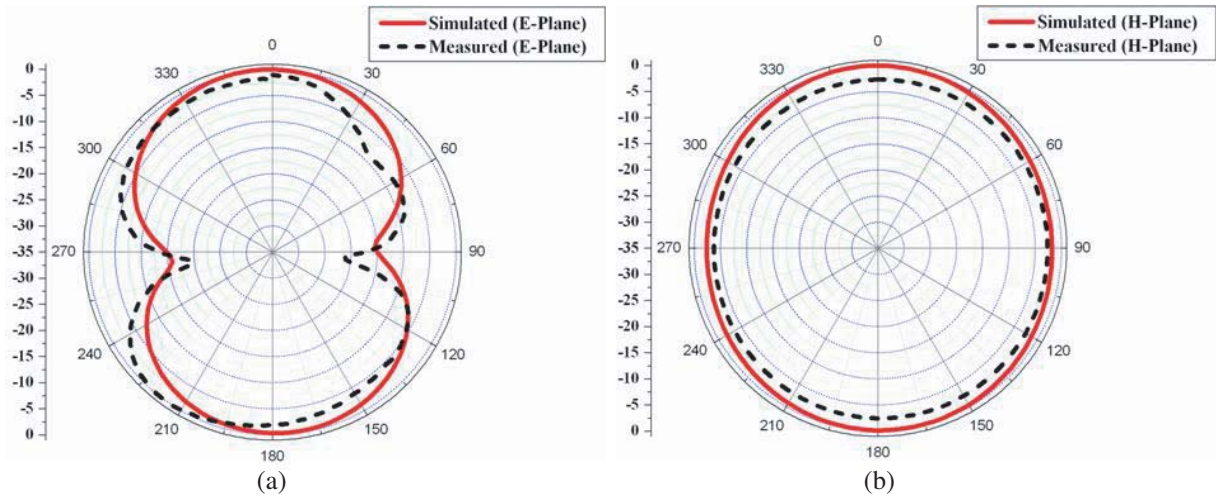$$\omega_r = \sqrt{\frac{3d}{\pi^2 r}} \left(\frac{C}{r} \right) \tag{4}$$

Figure 12. E-plane and H-plane radiation patterns of the prototype antenna at 5.8 GHz.
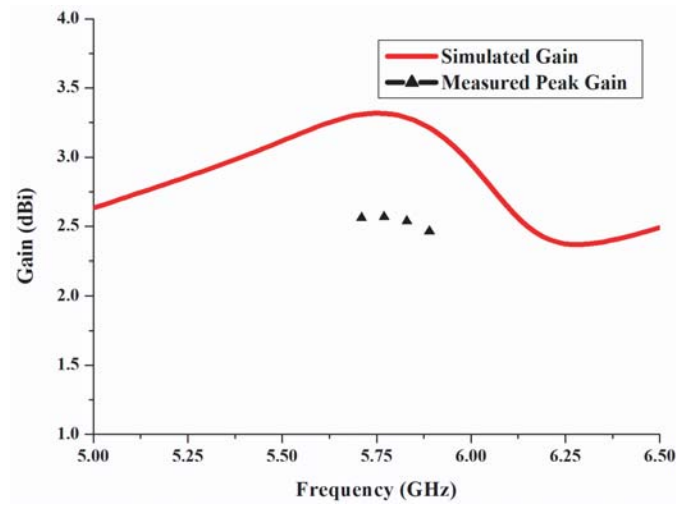

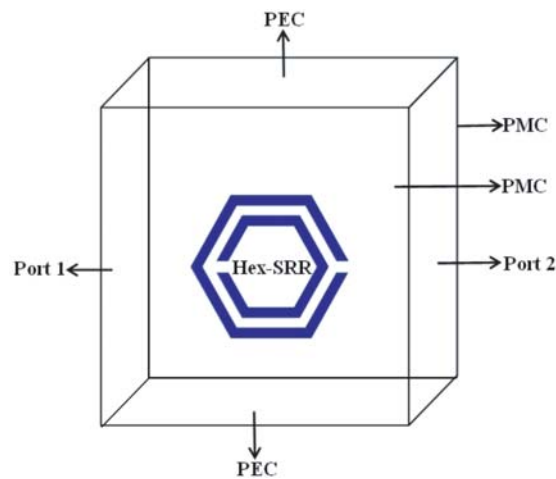**Figure 13.** Gain of the proposed antenna.
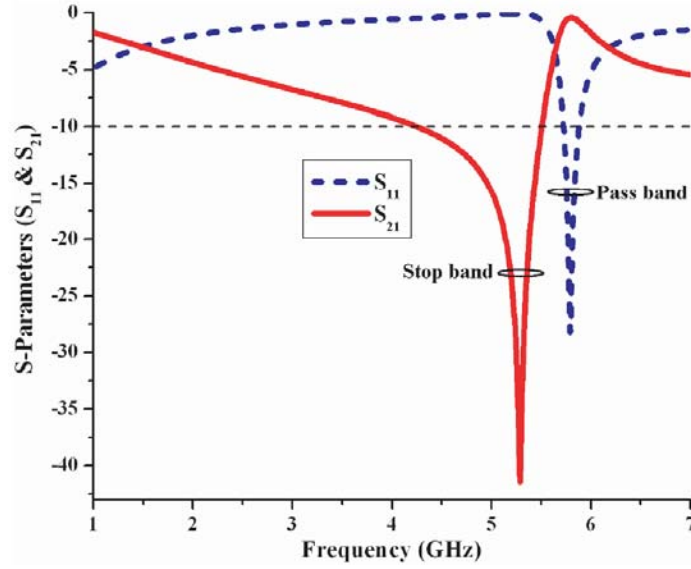

Figure 14. Waveguide setup to retrieve S-parameters.

Figure 15. S-parameters (S_{11} and S_{21}) of proposed Hex-SRR.
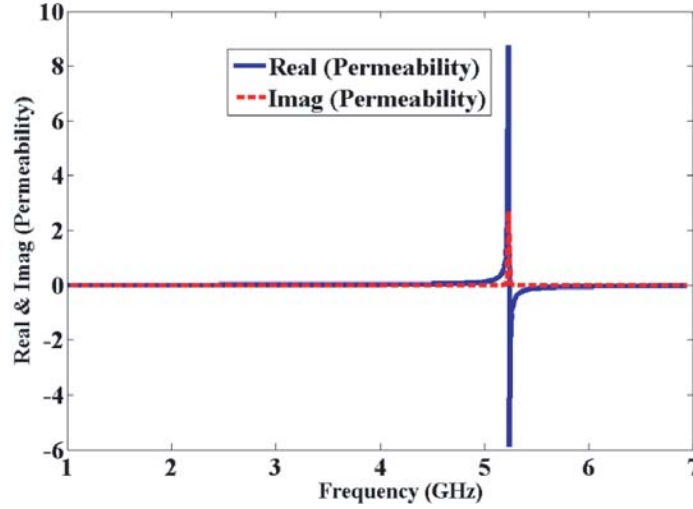

Figure 16. Extracted negative permeability of Hex-SRR at 5.3 GHz.

Here 'C' is the velocity of the light, 'd' the distance between the two rings, and 'r' the average side length of the inner Hex-SRR and outer Hex-CSRR. Substituting the values $d = 0.5$ mm and $r = 2.3$ mm in the above equation, we get $\omega_r = 33.55$ rad/sec, so $f_r = 5.34$ GHz. Therefore, the stopband (S_{21}) of proposed Hex-SRR is 5.3 GHz. Similarly, the passband (S_{11}) of Hex-SRR is inferred at 5.8 GHz within the frequency range of (5.47–6.06 GHz). Thus, the narrow passband of Hex-SRR constructs the new resonance frequency of 5.8 GHz in the return loss characteristics of the proposed antenna.

The negative permeability (μ) occurs at 5.3 GHz due to stopband behavior as shown in Fig. 16, which is computed by Nicolson Ross Weir (NRW) equations [10].

$$\varepsilon_r = \frac{2}{jk_0 d} * \frac{1-V_1}{1+V_1} \tag{5}$$

$$\mu_r = \frac{2}{jk_0 d} * \frac{1-V_2}{1+V_2}$$

where $V_1 = S_{21} - S_{11}$, $V_2 = S_{21} + S_{11}$, k_0 = Wave number of free space, d = substrate thickness.

8. CONCLUSION

A split ring monopole antenna loaded with Hex-SRR is proposed for 5.8 GHz RFID applications. It is exposed that Hex-SRR loaded in the split ring radiating element accounts for the optimum performance of the antenna in WLAN/RFID 5.8 GHz applications. The band characteristics of Hex-SRR are achieved by waveguide theory approach to confirm its metamaterial property at 5.3 GHz. The fabricated antenna has an electrical size of $0.4062\lambda_0 \times 0.4062\lambda_0 \times 0.031\lambda_0$, and its experimental data cover substantial radiation characteristics for RFID applications.

REFERENCES

1. Rajabloo, H., V. A. Kooshki, and H. Oraizi, "Compact microstrip fractal Koch slot antenna with ELC coupling load for triple band application," *AEU Int. J. Electron C*, Vol. 73, 144–149, 2017.

2. Imaculate Rosaline, S. and S. Raghavan, "Split ring loaded broadband monopole with SAR reduction," *Microwave Opt. Technol. Lett.*, Vol. 58, 158–162, 2015.

3. Boopathi Rani, R. and S. K. Pandey, "A parasitic hexagonal patch antenna surrounded by same shaped slot for WLAN, UWB applications with notch at vanet frequency band," *Microwave Opt. Technol. Lett.*, Vol. 58, 2996–3000, 2016.

4. Pandeeswari, R., "A compact non-bianisotropic complementary split ring resonator inspired microstrip triple band antenna," *Progress In Electromagnetics Research C*, Vol. 81, 115–124, 2018.

5. Murugeshwari, B., R. Samson Daniel, and S. Raghavan, "A compact dual band antenna based on metamaterialinspired split ring structure and hexagonal complementary splitring resonator for ISM/WiMAX/WLAN applications," *Appl. Phys. A*, Vol. 125, 628, 2019.

6. Pandeeswari, R. and S. Raghavan, "Meandered CPW-fed hexagonal split ring resonator monopole antenna for 5.8 GHz RFID applications," *Microwave Opt. Technol. Lett.*, Vol. 57, 681–681, 2015.

7. Pandeeswari, R. and S. Raghavan, "Broadband monopole antenna with split ring resonator loaded substrate for good impedance matching," *Microwave Opt. Technol. Lett.*, Vol. 56, 2388–2392, 2014.

8. Yang, K., H. Wang, Z. Lei, Y. Xie, and H. Lai, "CPW-fed slot antenna with triangular SRR terminated feed line for WLAN/WiMAX applications," *Electron Lett.*, Vol. 47, 685–686, 2011.

9. Antoniades, M. A. and G. V. Eleftheriades, "A broadband dual-mode monopole antenna using NRI-TL metamaterial loading," *IEEE Antennas Wireless Propag. Lett.*, Vol. 8, 258–261, 2006.

10. Samson Daniel, R., R. Pandeeswari, and S. Deivalakshmi. "A CPW-fed dual band antenna based on metamaterial inspired split ring structure" *2017 IEEE 2nd International Conference on Signal and Image Processing*, 2017.

11. Samson Daniel, R., R. Pandeeswari, and S. Raghavan, "Multiband monopole antenna loaded with complementary split ring resonator and C-shaped slots," *AEU Int. J. Electron C*, Vol. 75, 8–14, 2017.

12. Immaculate, S. and S. Raghavan, "Design and analysis of a SRR superstrate for SAR reduction," *J. Electromagnet Wave*, Vol. 29, 2330–2338, 2015.

13. Samson Daniel, R., "Broadband negative antenna using ELC unit cell," *AEU Int. J. Electron C*, Vol. 118, 153147, 2020.

14. Balanis, C. A., *Modern Antenna Handbook*, A John Wiley and Sons, Inc., Publications, 2008.